

## Same sign di-lepton candles of the composite gluons

Aleksandr Azatov<sup>1\*</sup>, Debtoosh Chowdhury<sup>2†</sup>, Diptimoy Ghosh<sup>2,3‡</sup> and Tirtha Sankar Ray<sup>4§</sup>

<sup>1)</sup> *Theory Division, Physics Department, CERN, Geneva, Switzerland*

<sup>2)</sup> *INFN, Sezione di Roma, Piazzale Aldo Moro 2, I-00185 Rome, Italy*

<sup>3)</sup> *Department of Particle Physics and Astrophysics,  
Weizmann Institute of Science, Rehovot 7610001, Israel*

<sup>4)</sup> *Department of Physics, Indian Institute of Technology Kharagpur, 721 302, India*

### Abstract

Composite Higgs models, where the Higgs boson is identified with the pseudo-Nambu-Goldstone-Boson (pNGB) of a strong sector, typically have light composite fermions (top partners) to account for a light Higgs. This type of models, generically also predicts the existence of heavy vector fields (composite gluons) which appear as an octet of QCD. These composite gluons become very broad resonances once phase-space allows them to decay into two composite fermions. This makes their traditional experimental searches, which are designed to look for narrow resonances, quite ineffective. In this paper, we as an alternative, propose to utilize the impact of composite gluons on the production of top partners to constrain their parameter space. We place constraints on the parameters of the composite resonances using the 8 TeV LHC data and also assess the reach of the 14 TeV LHC. We find that the high luminosity LHC will be able to probe composite gluon masses up to  $\sim 6$  TeV, even in the broad resonance regime.

---

\* email: [aleksandr.azatov@cern.ch](mailto:aleksandr.azatov@cern.ch)

† email: [debtoosh.chowdhury@roma1.infn.it](mailto:debtoosh.chowdhury@roma1.infn.it)

‡ email: [diptimoy.ghosh@weizmann.ac.il](mailto:diptimoy.ghosh@weizmann.ac.il)

§ email: [tirthasankar.ray@gmail.com](mailto:tirthasankar.ray@gmail.com)

# Contents

<b>1</b>	<b>Introduction</b>	<b>2</b>
<b>2</b>	<b>The model setup</b>	<b>3</b>
<b>3</b>	<b>Analysis strategy</b>	<b>5</b>
<b>4</b>	<b>Details of collider simulation</b>	<b>6</b>
<b>5</b>	<b>Results</b>	<b>7</b>
<b>6</b>	<b>Conclusion</b>	<b>9</b>
<b>A</b>	<b>Event selection criteria</b>	<b>11</b>
A.1	ATLAS : 8 TeV . . . . .	11
A.2	CMS : 8 TeV . . . . .	12
A.3	14 TeV projections . . . . .	13
<b>B</b>	<b>Kinematics</b>	<b>13</b>
<b>C</b>	<b>Minimal composite Higgs model M4<sub>5</sub></b>	<b>14</b>

## 1 Introduction

The discovery of the Higgs boson at the Large Hadron Collider (LHC) [1, 2] has propelled us to the era of Higgs property measurements. Whether the discovered Higgs boson is an elementary or a composite object is an outstanding question, and would be at the cynosure of attention in the second run of the LHC which is about to start in a few months. In this context, models where the Higgs boson is a pNGB of a global symmetry spontaneously broken by a strongly coupled sector, represent well motivated scenarios of electroweak symmetry breaking containing a composite Higgs. [3–5] (see Ref. [6] for a recent review).

In the models where the Standard Model (SM) fermion masses are generated by the partial compositeness mechanism [7], the strong sector must contain fermionic colored resonances. These, so called, top partners, are crucial to ensure the finiteness of the SM fermion contributions to the radiatively generated potential for the pNGB Higgs [5, 8]. These resonances are expected to be light in order to reproduce the observed mass of the SM Higgs boson without introducing additional tuning into the model [9–13], and their direct search at the LHC [14, 15] already constrains them to be heavier than  $\gtrsim 800$  GeV.

Since the top partners are coloured, generically one expects the presence of coloured vector resonances as well. In this paper we focus on the indirect constraints on the composite vector fields (composite gluons) which are in the adjoint representation of  $SU(3)_{\text{Color}}$ . They can be identified with the Kaluza-Klein (KK) excitation of the SM gluons in the five-dimensional realizations of the composite scenarios [5]. The two loop contribution of these composite gluons to the Higgs potential is known to soften the fine-tuning in these models [16]. However, the low energy flavour violating observables, especially  $\epsilon_K$  in the  $K^0 - \bar{K}^0$  system, were shown to strongly prefer the mass of the composite gluon to be  $m_\rho \gtrsim 10 - 30$  TeV [17–20], thus making it impossible to produce them at the LHC. Introduction of flavour symmetries [21–26] can make these vector resonances light while being compatible with the flavour observables. In this work, however, we will not rely on any additional symmetries in the flavour sector and assume that there are cancellations among different contributions, allowing the composite gluons to be light and hence, accessible at the LHC.

If the decay of the composite gluon to the top partners is kinematically allowed, typically large couplings of the strong sector imply that the composite gluon will have large width, comparable to its mass. In that case, the traditional approach to search for heavy gluons through resonance hunting may prove ineffective [27]. However, as we will elaborate in this work, these broad resonances can be cornered by several other (cut-and-count) searches being carried out at the LHC. In particular, the gluon partners contribute to the top partner pair production cross-section and this can be used to put useful constraints on them [27]<sup>1</sup>. In this paper we adopt this approach and recast the studies carried out to search for top partners to constrain the composite gluon parameter space. In particular, our study will focus on the indirect bounds on the parameter space of the composite gluons from the top partner searches with the same sign dilepton final state by the ATLAS [28] and CMS [29] collaborations<sup>2</sup>. We will also study the reach of the 14 TeV LHC. Recently this strategy was also used in the phenomenological study of Ref. [30], which however was focused on the parameter space with a narrower decay width of the composite gluon. For some other related studies, we refer the reader to Refs. [31–37].

The rest of this paper is organized as follows. In Section 2 we will present the Lagrangian of our simplified model and briefly discuss the branching ratios of the composite gluon to various top partners. In Section 3 we will discuss the subtleties involved in dealing with broad resonances. The details of our numerical simulation will be presented in section 4. We will present our main results in section 5 and conclude thereafter.

## 2 The model setup

In this section we present the basic structure of our model. We assume that the global symmetry breaking pattern leading to the pNGB Higgs is given by the  $SO(5)/SO(4)$  coset. This is the minimal coset that contains an unbroken custodial symmetry. We will assume that the SM fermion masses are generated by the partial compositeness mechanism. The simplified two-site construction [40] will be utilized to describe the phenomenology of the lightest composite resonances. In particular, we will be interested in the phenomenology of the fermionic top partners and the partner of the SM gluon - the composite gluon and we will ignore the rest of the composite resonances. For concreteness we focus on the  $M_{45}$  model presented in [41], minimally extended by the inclusion of the composite gluon. In this setup the top partners belong to the  $\mathbf{4}$  of  $SO(4)$  appearing as a part of  $\mathbf{5}$  of

<sup>1</sup>In principle this type of analysis can be used even for the narrow resonance searches however, if the resonance is within the kinematic reach bump-hunting may be a better search strategy.

<sup>2</sup>While we considered only the same-sign di-lepton channel in our analysis, there are also other channels (e.g., final state with top quarks decaying hadronically) which can be potentially important [38, 39].

$SO(5)$ .<sup>3</sup> The relevant Lagrangian is given by

$$\mathcal{L}^{\mathbf{M4}_5} \supset -M_Q \bar{Q}Q + yf(\bar{\Psi}_L)^I U_{Ii} \mathcal{Q}_R^i + yc_2 f(\bar{\Psi}_L)^I U_{I5} t_R, \quad (1)$$

where  $Q$  is the composite multiplet in the representation  $\mathbf{4}$ , the  $\Psi_L$  contains the SM left-handed quark doublet and  $U_I$  is the non-linear representation of the pNGB Higgs and  $t_R$  is assumed to be a fully composite state. Generically the lightest state is the field with charge  $5/3$ . One of the interesting features of this particle is that it decays with 100% branching ratio into the  $tW$  final state which, after the further decay of the top quark, leads to the same sign di-lepton final state. This interesting feature was used recently in the experimental studies to put bound on the mass of the fermionic top partners,  $M_{5/3} \gtrsim 800$  GeV [29]. Note that this bound was obtained assuming only the QCD pair production of the charge  $5/3$  field. Later it was realized that the electroweak single production of the charge  $5/3$  field can also lead to the same final state, thus making the overall bound even stronger [41, 43].

In this paper we follow a very similar approach and study the constraints from the additional mechanism for pair production of the charge  $5/3$  field namely, processes mediated by the composite gluons. Note that in the model  $\mathbf{M4}_5$  we have one state with charge  $5/3$ , one state with charge  $-1/3$  and two top-like states with electric charge  $2/3$ . We will denote these states by  $X_{5/3}$ ,  $B_{-1/3}$ ,  $T_{2/3}^1$  and  $T_{2/3}^2$  respectively (see Appendix C for the details of the model setup).

The interaction of the composite gluons can be read off from the two-site model of the Ref. [40] and is given by,

$$\begin{aligned} \mathcal{L}_{gauge} = & g_{QCD} A_\mu (\bar{Q}\gamma^\mu Q + \bar{\Psi}_L\gamma^\mu\Psi_L + \bar{t}_R\gamma^\mu t_R) \\ & + \rho_\mu \left[ \sqrt{g_*^2 - g_{QCD}^2} (\bar{Q}\gamma^\mu Q + \bar{t}_R\gamma^\mu t_R) - \frac{g_{QCD}^2}{\sqrt{g_*^2 - g_{QCD}^2}} \bar{\Psi}_L\gamma^\mu\Psi_L \right]. \end{aligned} \quad (2)$$

Hence, the interaction of the composite gluon  $\rho$  in the limit  $g_* \gg g_{QCD}$  can be written as

$$\approx \rho_\mu \left[ g_* (\bar{Q}\gamma^\mu Q + \bar{t}_R\gamma^\mu t_R) - \frac{g_{QCD}^2}{g_*} \bar{\Psi}_L\gamma^\mu\Psi_L \right]. \quad (3)$$

Similarly the couplings between the other SM fermions (which we assume to be elementary) and the composite gluon are equal to

$$- \frac{g_{QCD}^2}{\sqrt{g_*^2 + g_{QCD}^2}} \approx - \frac{g_{QCD}^2}{g_*}. \quad (4)$$

One can see that the coupling of the elementary fermions to the composite gluon is suppressed (compared to the coupling to the SM gluon) by the factor  $\frac{g_{QCD}}{g_*}$  which can be calculated in the explicit warped five-dimensional models and is given by  $\frac{g_*}{g_{QCD}} \sim \sqrt{\log \frac{M_{\text{Pl}}}{\text{TeV}}} \sim 6$  [44]. Note that Eq. 2 is written in the two-site basis, before the diagonalization of the fermion mass matrix. The elementary left-handed top quark mixes strongly with the composite sector due to the  $yf$  term in the Lagrangian, see Eq. 1, and it is convenient to introduce the parameter (sine of the mixing angle between  $t_L$  and composite fields in the absence of the electroweak symmetry breaking),

$$s_L \equiv \frac{f^2 y^2}{\sqrt{f^2 y^2 + M_Q^2}}, \quad (5)$$

<sup>3</sup>This is the minimal construction which has a custodial protection for the large modifications of the  $Z\bar{b}_L b_L$  coupling [42].

to measure of compositeness of the left-handed top.

Let us summarize some basic properties of the composite gluons that are important for phenomenology [40]. Throughout this paper we will assume that all the light quarks (except for the bottom) are elementary. Thus, the dominant production of the composite gluon ( $\rho$ ) will be by the process  $q\bar{q} \rightarrow \rho$  with the coupling constant  $\frac{g_{QCD}^2}{\sqrt{g_*^2 - g_{QCD}^2}}$ . Once produced,  $\rho$  will decay predominantly into composite states due to the large coupling constant  $g_*$ . In this work we will assume that only the SM fermions of the third generation mix strongly with the composite sector<sup>4</sup>. The channels contributing to the signal in the same sign di-lepton final state, with some typical values of the branching fractions are given by:

$$\begin{aligned}
& pp \rightarrow \rho \rightarrow X_{5/3}\bar{X}_{5/3}(X_{5/3} \rightarrow tW) \\
& Br(\rho \rightarrow X_{5/3}\bar{X}_{5/3}) \sim 0.2 - 0.25, \quad Br(X_{5/3}\bar{X}_{5/3} \rightarrow \text{same sign leptons}) \sim 0.09 \\
& pp \rightarrow \rho \rightarrow B_{-1/3}\bar{B}_{-1/3}(B_{-1/3} \rightarrow tW) \\
& Br(\rho \rightarrow B_{-1/3}\bar{B}_{-1/3}) \sim 0.07 - 0.15, \quad Br(B_{-1/3}\bar{B}_{-1/3} \rightarrow \text{same sign leptons}) \sim 0.09 \\
& pp \rightarrow \rho \rightarrow T_{2/3}\bar{T}_{2/3}(T_{2/3} \rightarrow tZ, T_{2/3} \rightarrow th), \\
& Br(\rho \rightarrow T_{2/3}^1\bar{T}_{2/3}^1) \sim 0.08 - 0.15, \quad Br(\rho \rightarrow T_{2/3}^2\bar{T}_{2/3}^2) \sim 0.2 - 0.25, \\
& Br(T_{2/3}\bar{T}_{2/3} \rightarrow \text{same sign leptons}) \sim 0.02.
\end{aligned} \tag{6}$$

It can be seen that the same sign di-lepton (electrons and muons only) final state will get the dominant contributions from the 5/3 and  $-1/3$  fields. The contribution of the top-like fields is not negligible, however it is much smaller than the effect of the 5/3 field and hence, we ignore them in our analysis. The other major branching ratios for the composite gluon are:

$$\begin{aligned}
& Br(\rho \rightarrow T_{2/3}^2 t) \sim 0.03 - 0.06, \quad Br(\rho \rightarrow tt) \sim 0.11 - 0.2 \\
& Br(\rho \rightarrow B_{-1/3} b) \sim 0.01 - 0.05, \quad Br(\rho \rightarrow bb) \sim 0.01 - 0.07.
\end{aligned} \tag{7}$$

### 3 Analysis strategy

As we mentioned before, the goal of our study is to find the constraints coming from composite gluon mediated contribution to the top partner pair production. However, owing to the large coupling the decay width of the composite gluon is often comparable to its mass in the large region of the parameter space we are interested in. This invalidates the approximation of a narrow Breit-Wigner resonance for computation of the cross section (for earlier studies of the wide width effects of the composite gluon resonances, see Refs. [46–48]). Indeed the partonic cross section is proportional to

$$\sigma(\hat{s}) \propto \frac{1}{(\hat{s} - M_\rho^2)^2 + (\text{Im}[M^2(\hat{s})])^2}, \tag{8}$$

where  $-iM^2(\hat{s})$  is the sum of all one-particle-irreducible insertions into the  $\rho$  propagator. In the limit  $M_\rho \gg \Gamma_\rho$  the cross section is dominated by the on-shell  $\rho$  exchange and Eq. 8 reduces to the standard Breit-Wigner formula by substituting

$$-i\text{Im}[M^2(\hat{s})] \Rightarrow -\text{Im}[M^2(\hat{s} = M_\rho^2)] = M_\rho \Gamma_\rho. \tag{9}$$

<sup>4</sup>Generically the composite gluons can decay also to the partners of the light quarks thus reducing the  $Br(\rho \rightarrow \text{top partners})$ , however, as shown in [45], even these fields (partners of light quarks) in the anarchic scenarios are coupled predominantly to the third generation SM fields, so the similar analysis will be relevant.

In Appendix B we report the formula of  $\text{Im}[M^2(\hat{s})]$  and discuss the situation when the narrow width approximation is expected to fail. Instead of performing the full simulation with the true propagator shown in Eq. 8, we have divided our analysis into two parts. At first, we numerically calculate the total cross section using the exact formula of the propagator for every point in the relevant parameter space of the model. In the next step, in order to calculate the cut acceptance efficiencies, we first perform Monte Carlo simulation (including parton shower and hadronization) using Madgraph/Pythia (see the following section for more details) in the narrow width approximation. We then estimate the finite width effects on the cut acceptance efficiencies in the following way:

- for every value of the composite fermion mass  $M_X$  we calculate the cut acceptance efficiencies for various values of the mass and width of the composite gluon. We denote it by  $\epsilon_{M_X}(M_\rho, \Gamma_\rho)$ .
- for every mass of the composite fermion  $M_X$  we find the minimal efficiency by varying  $(M_\rho, \Gamma_\rho)$ ,

$$\epsilon_{M_X}^{Min} = \text{Min}[\epsilon_{M_X}(M_\rho, \Gamma_\rho)]. \quad (10)$$

We use  $\epsilon_{M_X}^{Min}$  as a conservative estimate of the cut acceptance efficiency for the process of pair production (via composite gluon exchange) of the heavy fermions with mass  $M_X$ .

Our procedure of estimating the efficiencies is well justified because of the fact that for a given value of the partonic center of mass energy  $\sqrt{\hat{s}}$ , the angular distribution of composite fermion pair production is independent of whether the full propagator of Eq. 8 or the narrow-width approximation is used. The difference is just an overall factor, because the modification in going from the former (true propagator of Eq. 8) to the latter (narrow Breit-Wigner resonance) is entirely a function of the kinematic variable  $\hat{s}$ . So the only modification will appear in the  $\hat{s}$ -distribution which can be estimated by studying the distributions for various values of  $M_\rho$  and  $\Gamma_\rho$  (for a fixed  $M_X$ ). In order to estimate the error of this approximation we will also provide a comparison of the approximate efficiencies with the exact calculation for a few benchmark points.

## 4 Details of collider simulation

In this section we briefly describe the steps followed to perform the simulation and the event selection criteria used in our analysis. We have implemented the model in FeynRules 2.0 [49] and created the corresponding UFO files for the Madgraph event generator [50]. Madgraph 2.2.1 has been used to generate the parton level events. Subsequently the Madgraph-Pythia interface [51, 52] was utilized to perform the showering and hadronization of the parton level events and implementing our event selection cuts. The parton distribution function CTEQ6L [53] has been used throughout our analysis. We have employed the Fastjet3 package [55–57] for reconstruction of the jets and implementation of the jet substructure analysis used for the reconstructing the top quarks and  $W$  bosons.

As our goal is to recast the CMS [29] and ATLAS [28]<sup>5</sup> searches for the charge-5/3 top-quark partners in the same sign di-lepton final state, we have tried to follow their event selection procedures as closely as possible. For completeness, we present the step-by-step details of our analysis in appendix A.

We find that the cut acceptance efficiency varies in the range 0.019 – 0.028 for both the ATLAS and CMS 8 TeV analyses (our efficiencies include the branching ratio of  $W$  boson into leptons). For the 14 TeV analysis we find that the efficiency varies between 0.009 and 0.013.

<sup>5</sup>While this work was close to its completion, a new analysis by the ATLAS collaboration appeared [54] which found a slightly stronger lower bound on the mass of charge 5/3 top partner,  $M_{5/3} \gtrsim 840$  GeV.

## 5 Results

In this section we will present the final results of our study. We start by analyzing the current LHC constraints on the composite gluons. Both the ATLAS and CMS collaborations have reported the exclusion limits on the QCD pair production of the fermionic top partners. In order to constrain the heavy composite gluons, we recast their results in the following way: we consider that a point in the parameter space of the model is excluded if the number of events predicted by the model  $N_{\text{model}}$  is larger than the 95% C.L. exclusion limit reported by the experimental collaborations. In our analysis we ignore the interference between the composite gluon mediated pair production and the SM gluon contribution. This is a good approximation since the cross section is dominated by the on-shell  $\rho$  production and only the  $q\bar{q}$  initial state contributes to the  $\rho$  mediated processes<sup>6</sup>.

As we have argued in the previous section, in order to accurately calculate the total cross section due to the wide resonances one needs to know  $\text{Im}[M^2(\hat{s})]$  for all values of  $\hat{s}$  and *not only* on the mass peak. This requires the full knowledge of the masses of the particles and their couplings in the range of interest of  $\hat{s}$ , which makes it impossible to obtain completely model independent constraints. In this paper, as mentioned before, we have decided to focus on the  $M4_5$  model, which is the simplest composite Higgs construction containing charge  $5/3$  and  $-1/3$  fields. The model given in Eq. 1-2 can be parametrized in terms of the five independent parameters,  $M_\rho$ ,  $M_Q$ ,  $s_L$ ,  $g_*$  and  $f$ . In our numerical simulations we set  $f = 764$  GeV, which corresponds to 10% fine-tuning of the electroweak symmetry breaking scale. The parameter  $c_2$  is fixed by requiring that the correct top quark mass is reproduced (see Eq.18).

In our calculation we consider the same sign di-lepton state originating from the QCD and composite gluon mediated pair production of the charge  $5/3$  and  $-1/3$  fields and we ignore the sub-dominant contribution of the charge  $2/3$  top partners.

The QCD pair production cross section was calculated using HATHOR [58] at NNLO. For the composite gluon mediated contribution, we however used the Leading Order (LO) cross section. Note that, the higher order corrections to the QCD pair production lead to an increase in the pair production cross section (see, for example [59]) with the corresponding  $K$ -factors  $\sim 1.5$ . Assuming that a similar increase happens also for the composite gluon mediated contribution, our use of LO cross section gives an conservative estimate of the expected bounds.

The exclusion plots presented in the Fig. 1-4 are obtained using the approximate efficiencies  $\epsilon_{M_X}^{\text{Min}}$  defined in Eq. 10. However we crosschecked them against the true efficiencies for a few reference points using the modified version of the Madgraph/Pythia interface, where the full energy dependence of the composite gluon propagator was included. The results are presented in the Table 1. One can notice that our method leads to a conservative estimate of the acceptance efficiencies and the difference between the true and approximate efficiencies is always within 25%, thus justifying the use of the latter ones.

Let us start by looking at the current bounds from the LHC searches. In Fig. 1 we show the exclusion contours in the  $M_\rho - M_X$  plane for a fixed value of left-handed top compositeness,  $s_L = 0.5$ . Similar exclusion contours in the  $s_L - M_X$  plane are shown in Fig. 2 for two fixed values of  $M_\rho$ ,  $M_\rho = 2.5$  TeV and  $M_\rho = 3$  TeV. We find that the limits on the composite gluon mass relax substantially below the narrow width limit of 2.5 TeV [60,61] once the decay channels into the composite top partners becomes open. However, the current searches for the top partners still lead to interesting constraints on the composite gluons in the mass range of 2-3 TeV, for the medium large composite gluon coupling  $g_* \in [2, 3]$  and the width  $\Gamma_\rho \sim (0.1 - 0.4)M_\rho$ . For the smaller values

---

<sup>6</sup>In our analysis we have ignored the contribution of the single production of the composite fermions studied in [39,41,43]

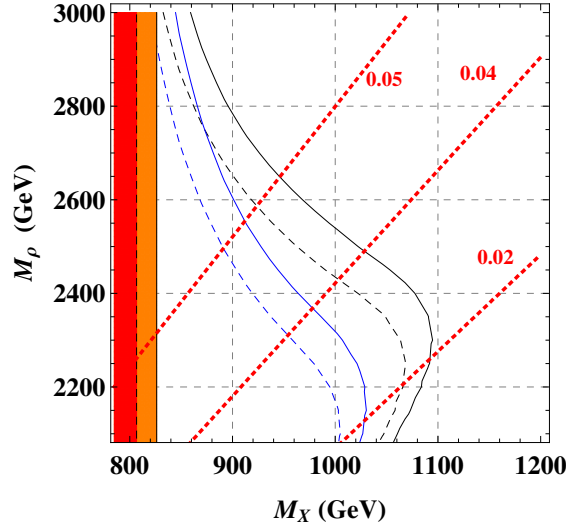


Figure 1: 95% C.L. exclusion contours in the  $M_\rho - M_X$  plane for fixed value of  $s_L = 0.5$ . Solid lines represent the constraints obtained from recasting the CMS study and the dashed lines correspond to the ones from the ATLAS study. The black (blue) lines correspond to the value  $g_* = 2.5(3)$ . The red dotted lines indicate the ratio  $\frac{\Gamma_\rho}{M_\rho} \times \left( \frac{1}{g_*^2 - g_{QCD}^2} \right)$ . The orange and red vertical bands are the constraints from the CMS [29] and ATLAS [28] searches respectively assuming only QCD production.

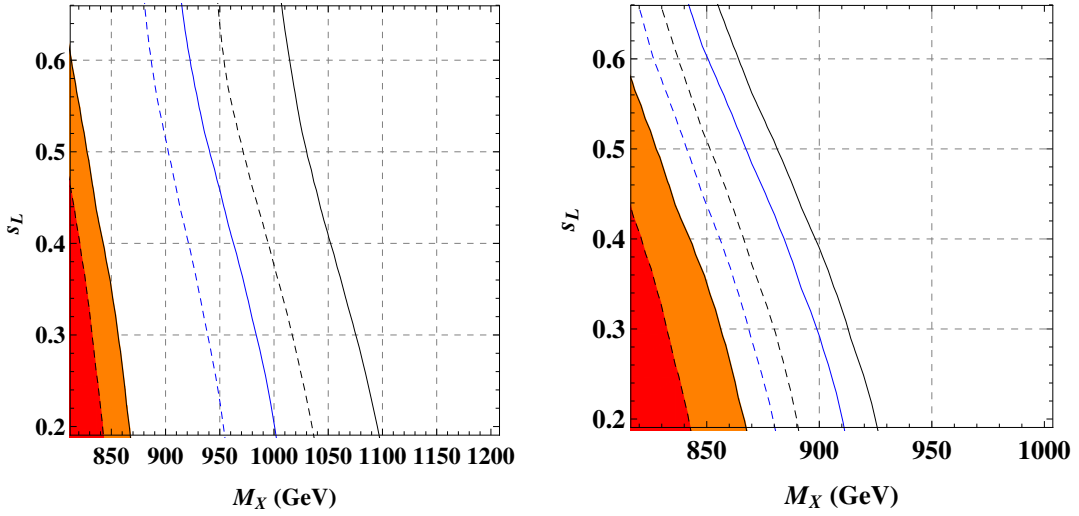


Figure 2: 95 % C.L. exclusion contours in the  $s_L - M_X$  plane for two fixed value of  $M_\rho$ ,  $M_\rho = 2.5$  TeV (left panel) and  $M_\rho = 3$  TeV (right panel). Solid lines represent the constraints obtained from recasting the the CMS study and the dashed lines correspond to the ones from the ATLAS study. The black (blue) lines correspond to the value  $g_* = 2.5(3)$ . The orange and red bands are the constraints from the CMS [29] and ATLAS [28] searches respectively assuming only QCD production.



Reference points for 8 TeV LHC	CMS 5/3	ATLAS 5/3	CMS -1/3	ATLAS -1/3
$M_\rho = 2.5$ TeV, $M_X = 1$ TeV, $g_* = 2.5$	0.023(0.022)	0.023(0.023)	0.028 (0.024)	0.025(0.023)
$M_\rho = 2.5$ TeV, $M_X = 0.9$ TeV, $g_* = 3$	0.025 (0.02)	0.023(0.022)	0.025 (0.22)	0.024 (0.023)
$M_\rho = 2.2$ TeV, $M_X = 0.9$ TeV, $g_* = 3$	0.024 (0.02)	0.024(0.022)	0.026(0.22)	0.024(0.023)
Reference points for 14 TeV LHC	5/3	-1/3		
$M_\rho = 5.5$ TeV, $M_X = 2$ TeV, $g_* = 3$	0.016 (0.013)	0.015 (0.012)		
$M_\rho = 5$ TeV, $M_X = 2$ TeV, $g_* = 4$	0.015 (0.013)	0.016(0.012)		
$M_\rho = 4.5$ TeV, $M_X = 2$ TeV, $g_* = 4$	0.015 (0.013)	0.016 (0.012)		

Table 1: The comparison between the true efficiencies and the  $\epsilon_{M_X}^{Min}$  (in parenthesis) defined in Eq. 10. The mixing between left-handed top quark and composite fermions was set  $s_L = 0.5$  for all the reference points.

of the coupling  $g_*$  narrow resonance searches will become the most important tool in constraining the new colored resonances and for the larger  $g_*$ , the composite gluon contribution becomes sub-dominant.

**LHC 14 TeV reach:** In order to estimate the discovery reach at the 14 TeV LHC we have adopted the analysis presented in Ref. [62]. We again present our results as 95% C.L. exclusion contours in the  $M_\rho - M_X$  plane (Fig. 3) and  $s_L - M_X$  plane (Fig. 4). It can be noticed that composite gluons up to the masses  $\lesssim 6$  TeV and the fermions masses up to  $\sim 2.1$  TeV can be probed for  $g_* \sim 3 - 4$ . One can see from Fig. 3 that we can easily probe the composite gluons with the decay width as large as 1 TeV, the parameter space which is not covered by the narrow resonance searches.

Even though the expected 14 TeV constraints are weaker than the current bounds from the flavour violating observables (e.g.,  $\epsilon_K$ ), one should notice that unlike flavour violating observables which scale as  $\frac{1}{M_*^2}$  [18] the collider constraint gets stronger for smaller values of  $g_*$  (for fixed value of  $M_*$ ), leading to complementary constraints for small/medium  $g_*$ . We would also like to comment that for a highly composite  $t_L$  the left-handed bottom quark  $b_L$  becomes composite as well and can give an important contribution to  $pp \rightarrow \rho$  process due to the bottom parton density function. However, we find that this effect can contribute at most as

$$\frac{\sigma(pp(b\bar{b}) \rightarrow \rho)}{\sigma(pp(q\bar{q}) \rightarrow \rho)} \lesssim 2\% \left(\frac{g_*}{4}\right)^4 \left(\frac{s_L}{\sqrt{2}}\right)^4, \quad (11)$$

which is just a few percent for the values of the  $g_*$  and  $s_L$  we used in our study.

## 6 Conclusion

In this paper we have studied the collider phenomenology of the composite gluon within a composite Higgs model framework. Our study focused on the region of the parameter space where the composite gluon is kinematically allowed to decay into two fermionic top partners. In this region, typically the width of the composite gluons is expected to be comparable to its mass thus rendering the traditional resonance searches less effective [30]. However, as pointed out in [27], the contribution of the composite gluon to the pair production of two top partners can be still significant. In this context, we have studied the current constraints as well as high luminosity LHC prospects on the composite gluon using the additional contribution to the top partner pair production mediated by the heavy gluon. As the calculation of the composite gluon contribution to the top partner pair production cross section required knowledge of the full spectrum of the composite fields, we have

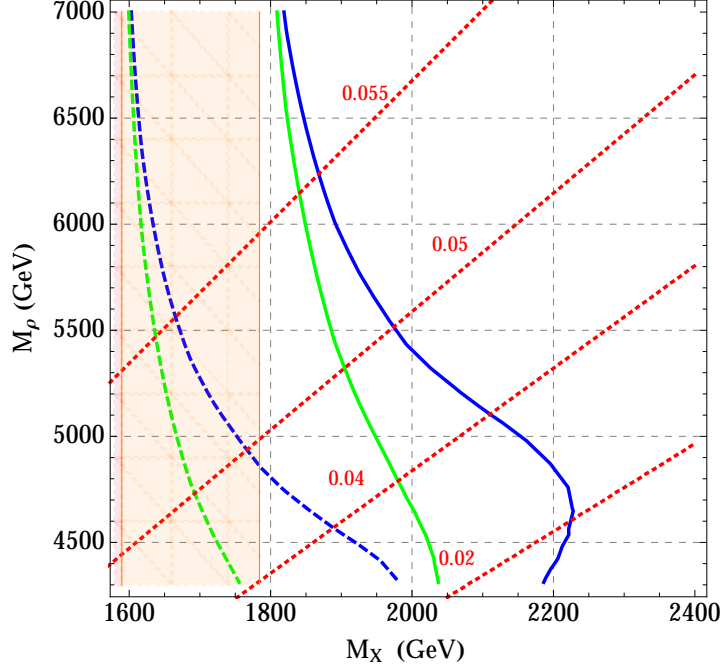


Figure 3: Prospects of the 95% C.L. exclusion contours in the  $M_\rho - M_X$  plane for fixed value of  $s_L = 0.5$ . The dashed (solid) lines represent LHC 14 exclusion reach for an integrated luminosity of  $300 \text{ fb}^{-1}$  ( $3 \text{ ab}^{-1}$ ). The blue (green) line corresponds to the value  $g_* = 3(4)$ . The red dotted lines indicate the ratio  $\frac{\Gamma_\rho}{M_\rho} \times \left( \frac{1}{g_*^2 - g_{QCD}^2} \right)$ . The red (orange) region is the exclusion prospects solely from QCD pair production at  $300 \text{ fb}^{-1}$  ( $3 \text{ ab}^{-1}$ ).

chosen for simplicity to exclusively focus only on the model  $M4_5$ . In our analysis, we have calculated the total cross section treating carefully the finite width effects and we have performed a detailed collider simulations in order to find a conservative estimate of the cut acceptance efficiencies.

We found that while the current data probes the composite gluon in the mass range  $2 - 3 \text{ TeV}$ , the high luminosity LHC will expectedly do much better and the exclusion limits can be extended to composite gluon masses of  $\sim 6 \text{ TeV}$  approaching very close to the mass range motivated by the flavour physics constraints.

## Acknowledgements

We would like to thank K.Agashe, G.Panico and G.Perez for comments on the manuscript and R. Contino for discussion. We would like to acknowledge the hospitality of the Centro de Ciencias de Benasque Pedro Pascual where this project was envisaged. DC and DG acknowledge support from the European Research Council under the European Union's Seventh Framework Program (FP/2007-2013)/ERC Grant Agreement No. 279972. The work of TSR is supported by INSPIRE faculty grant DST, Govt. of India and ISIRD grant IIT-Kharagpur, India.

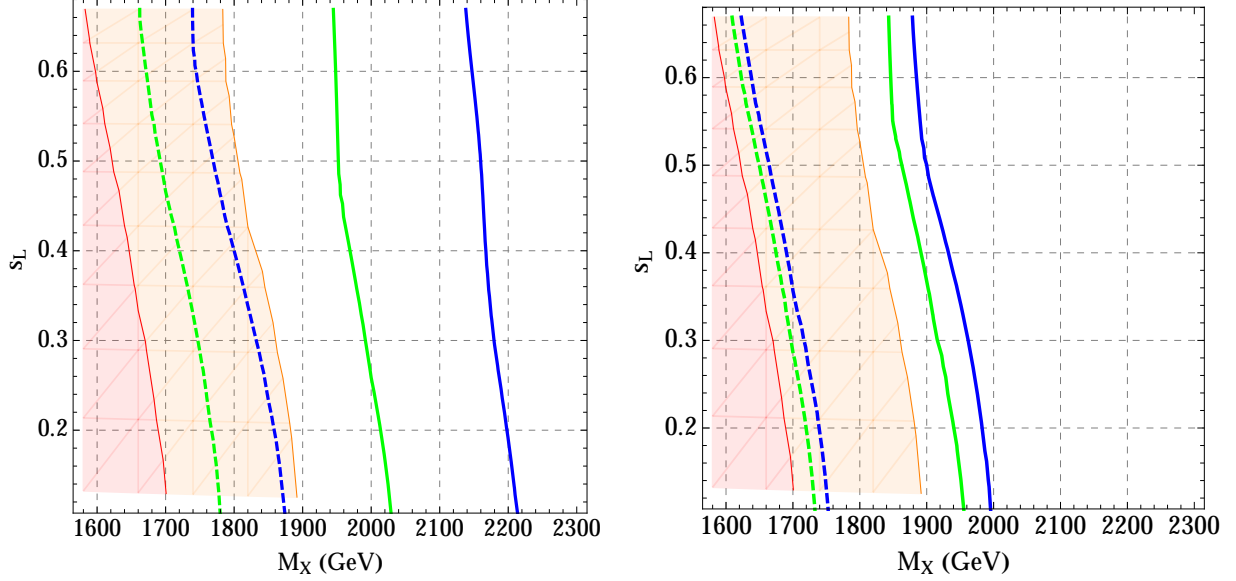


Figure 4: Prospects of the 95% C.L. exclusion contours in the  $s_L - M_X$  plane for for two fixed value of  $M_\rho$ ,  $M_\rho = 5$  TeV (left panel) and  $M_\rho = 6$  TeV (right panel). The dashed (solid) lines represent LHC 14 exclusion reach for an integrated luminosity of  $300 \text{ fb}^{-1}$  ( $3 \text{ ab}^{-1}$ ). The blue (green) line corresponds to the value  $g_* = 3(4)$ . The red (orange) region is the exclusion prospects solely from QCD pair production at  $300 \text{ fb}^{-1}$  ( $3 \text{ ab}^{-1}$ ).

## A Event selection criteria

In this appendix we present the details of our cut-and-count analysis used for recasting the ATLAS [28] and CMS [29] 8 TeV results, and also the 14 TeV projection from [62].

### A.1 ATLAS : 8 TeV

- Selection-I : An event is accepted only if it has exactly two leptons (electron or muon), both with the same electric charge. All leptons are selected with a transverse momentum cut  $p_T^\ell \geq 24$  GeV and the pseudo-rapidity  $|\eta| \leq 2.4$ . Moreover, the region of pseudo-rapidity  $1.37 < |\eta| < 1.52$  is excluded. Leptons are also required to satisfy the following isolation criteria,
  - (i) the distance between the lepton and any of the jets,  $\Delta R(j \ell)$ , must satisfy  $\Delta R > 0.4$  (see below for the details of jet reconstruction)
  - (ii) the lepton should be far enough from all the other leptons,  $\Delta R(\ell \ell) > 0.35$
  - (iii) the ratio of the total hadronic transverse energy deposit within a cone of  $\Delta R = 0.35$  around the lepton to the lepton transverse energy is  $\leq 5\%$ .
- Selection-II : If the same sign leptons are of electron flavour ( $e^+e^+$  or  $e^-e^-$ ), their invariant mass ( $m_{ee}$ ) is required to satisfy  $m_{ee} > 15$  GeV and  $|m_{ee} - m_Z| > 10$  GeV.

- Selection-III : Jets are constructed using the anti- $k_T$  [56] algorithm with the radius parameter  $R=0.4$ . Only those jets which satisfy  $p_T^j \geq 25$  GeV and the pseudo-rapidity  $|\eta| \leq 2.5$  are selected. We demand the presence of at least 2 such jets in every event.
- Selection-IV : Every event is required to have at least one  $b$ -tagged jet. A jet is identified as a  $b$ -jet if it is close ( $\Delta R < 0.2$ ) to a  $b$ -quark. For the  $b$ -tagging efficiency ( $\epsilon_b$ ) we use the prescription from reference [63] which gives  $\epsilon_b = 0.71$  for  $90 \text{ GeV} < p_T < 170 \text{ GeV}$  and at higher (lower)  $p_T$  it decreases linearly with a slope of  $-0.0004$  ( $-0.0047$ )  $\text{GeV}^{-1}$ . Moreover, the probability of mis-tagging a  $c$ -jet (light jet) as a  $b$ -jet is taken to be 20% (0.73%) [64].
- Selection-V : We define the effective mass of an event to be  $m_{\text{eff}} = \sum_j p_T^j + \sum_\ell p_T^\ell$  and demand that the event satisfies  $m_{\text{eff}} > 650$  GeV. Additionally, we also ask for a minimum missing transverse momentum  $\cancel{E}_T > 40$  GeV in every event.

## A.2 CMS : 8 TeV

- Selection-I : An event is accepted only if it has exactly two leptons (electron or muon), both with the same electric charge. All leptons are selected with a transverse momentum cut  $p_T^\ell \geq 30$  GeV and the pseudo-rapidity  $|\eta| \leq 2.4$ . Leptons are also required to satisfy the following isolation criteria,
  - (i) the distance between the lepton and any of the reconstructed top quarks must satisfy  $\Delta R > 0.8$  (see below for the details of top quark reconstruction)
  - (ii) the lepton should be far enough from all the other leptons,  $\Delta R(\ell \ell) > 0.35$
  - (iii) the ratio (the  $I_R$  threshold) of the total hadronic transverse energy deposit within a cone of  $\Delta R = 0.35$  around the lepton to the lepton transverse energy is  $\leq 17.5\%$ .
- Selection-II : If the same sign leptons are both electrons or both positrons, their invariant mass ( $m_{ee}$ ) is required to satisfy  $m_{ee} < 76$  GeV or  $m_{ee} > 106$  GeV.
- Selection-III : We construct “loose leptons” with a lower  $p_T^\ell$  cut of 15 GeV and relaxing the  $I_R$  threshold to 50%. Other selection criteria are kept identical to selection-I. We demand that all the same flavour opposite sign lepton pairs satisfy  $m_{\ell\ell} < 76$  GeV or  $m_{\ell\ell} > 106$  GeV.
- Selection-IV : The number of constituents ( $N_c$ ) in each event should satisfy  $N_c \geq 7$ , where  $N_c$  is defined as,

$$N_c = N_j + N_\ell + 2N_W + 3N_t. \quad (12)$$

Here  $N_j$  is the number of jets which are constructed using anti- $k_T$  algorithm with a distance parameter of 0.5 (AK5 jet). These jets are required to have  $p_T > 30$  GeV and  $|\eta| \leq 2.4$ . Moreover, they must be  $\Delta R > 0.3$  away from the leptons in selection-I and  $\Delta R > 0.8$  away from any other AK5 jet, reconstructed top quark and reconstructed  $W$  boson.  $N_\ell$  is the number of leptons counted from the same-sign di-leptons selected in selection-I.  $N_W$  and  $N_t$  refer to the total number of reconstructed top quarks and  $W$  bosons respectively.

- Selection-V :  $m_{\text{eff}} > 900$  GeV where  $m_{\text{eff}} = \sum_j p_T^j + \sum_\ell p_T^\ell$ . All the jets in the definition of  $m_{\text{eff}}$  must be at least  $\Delta R = 0.3$  away from the selected leptons and  $\Delta R = 0.8$  away from any other jet.

In order to reconstruct the top quarks we used the Johns Hopkins top tagger (JHTopTgger) [65] in our analysis. For the details of the steps followed in our simulation we refer the readers to section 3.2 of [66]. Here we briefly mention the differences compared to [66]. While constructing the fat-jets we used  $R = 0.8$ . Unlike

Ref. [66], we did not demand any limits on  $\delta_p$ ,  $\delta_r$  and  $\cos\theta_h$ . However, the fat-jet is required to have  $p_T > 400$  GeV and the pairwise invariant mass of the three highest  $p_T$  subjects is required to be greater than 50 GeV. The invariant mass of the subjects is required to be roughly consistent with the top mass, within the range 100 GeV - 250 GeV.

In order to reconstruct the  $W$  bosons we have used the algorithm proposed by Butterworth, Davison, Rubin, and Salam (BDRS) [67] to study the case of a light Higgs boson ( $m_H \sim 125$  GeV) produced in association with an electroweak gauge boson. For the step-by-step details of the algorithm, we refer our readers to Ref. [68]. The values of the parameters chosen in our analysis are exactly same to those used in Ref. [68] except the fact that we constructed the fat-jets with  $R = 0.8$  and asked for exactly 2 subjects in it. The fat-jets were also required to satisfy  $p_T > 200$  GeV. The two subjects should also have an invariant mass in the range 60 -100 GeV.

### A.3 14 TeV projections

- Selection-I : At least two same-sign leptons with  $p_T^\ell \geq 30$  GeV and the  $|\eta| \leq 2.4$ . The leading  $p_T$  lepton should also satisfy  $p_T^\ell \geq 80$  GeV. While checking lepton isolation we only impose the criteria (ii) and (iii) mentioned in the previous section.
- Selection-II : Same as Selection-II in the previous section.
- Selection-III : Same as Selection-III in the previous section.
- Selection-IV : The number of constituents  $N_c > 5$ , where  $N_c$  is defined in the same way as the previous section except that  $N_\ell$  now refers to the number of leptons (with  $p_T \geq 30$  GeV) excluding the two leptons used for the same-sign di-lepton requirement.
- Selection-V :  $m_{\text{eff}} > 1500$  GeV where  $m_{\text{eff}}$  is the scalar sum of the transverse momenta of all leptons and jets in the event with  $p_T > 30$  GeV. The missing transverse momenta  $\cancel{E}_T$  and the sum  $m_{\text{eff}} + \cancel{E}_T$  must also be more than 100 GeV and 2000 GeV respectively. Moreover, the leading and the second leading jets in transverse momentum are required to satisfy  $p_T > 150$  GeV and 50 GeV respectively.

We have used the same prescription as detailed in the previous section to tag the top quarks and the  $W$  bosons, the only difference being that the invariant mass of the subjects ( $m_{\text{inv}}$ ) are now required to satisfy  $140 < m_{\text{inv}} < 230$  GeV and  $60 < m_{\text{inv}} < 120$  GeV for top tagged jets and  $W$  tagged jets respectively.

## B Kinematics

In this section we will report some useful formulas for  $\rho$  production and decay. We will assume that the part of the Lagrangian responsible for the production and decay of  $\rho$  is given by,

$$\mathcal{L} \supset g_{\text{prod}} \bar{q} t^a \gamma^\mu q \rho_\mu^a + g_{\text{dec}} \bar{\chi}_1 t^a \gamma_\mu (1 + a_{12} \gamma_5) \chi_2 \rho_\mu^a. \quad (13)$$

The partonic cross-section of  $\bar{q}q \rightarrow \rho \rightarrow \bar{\chi}_1 \chi_2$  can be written as,

$$\hat{\sigma}(\hat{s}) = \frac{g_{\text{prod}}^2 g_{\text{dec}}^2}{54\pi \hat{s}} \frac{(\hat{s} - (m_{\chi_1} - m_{\chi_2})^2)^{\frac{1}{2}} (\hat{s} - (m_{\chi_1} + m_{\chi_2})^2)^{\frac{1}{2}}}{(\hat{s} - M_\rho^2)^2 + (\text{Im}[M^2(\hat{s})])^2} \times \left\{ (1 + |a_{12}|^2) \left[ \hat{s} - \frac{\hat{s}(m_{\chi_1}^2 + m_{\chi_2}^2) + (m_{\chi_1}^2 - m_{\chi_2}^2)^2}{2\hat{s}} \right] + 3m_{\chi_1} m_{\chi_2} (1 - |a_{12}|^2) \right\}. \quad (14)$$

Ref. points	$M_\rho, M_f, g_{decay}$	decay width	$\sigma_{True}$	$\sigma_{True}/\sigma_{NW}$
A	$M_\rho=3 \text{ TeV}, m_\chi=1.45 \text{ TeV}, g_{decay} = 5$	374 GeV	0.033 pb	0.9
B	$M_\rho=3 \text{ TeV}, m_\chi=1.2 \text{ TeV}, g_{decay} = 5$	788 GeV	0.061 pb	1.25
C	$M_\rho=3 \text{ TeV}, m_\chi=1 \text{ TeV}, g_{decay} = 2$	145 GeV	0.079 pb	1.01
D	$M_\rho=3 \text{ TeV}, m_\chi=1.495 \text{ TeV}, g_{decay} = 5$	121 GeV	0.029 pb	0.42

Table 2: Comparison of the true cross section  $\sigma_{True}$  with that obtained using narrow width approximation  $\sigma_{NW}$  (where  $-\text{Im}[M^2(\hat{s})]$  was substituted by  $\Gamma_\rho M_\rho$ ) for a few reference points. The coupling  $g_{prod}$  has been set to unity. The hadronic center of mass energy was set to be equal to  $\sqrt{S_{had}} = 8 \text{ TeV}$ .

One can now compute the hadronic cross section in proton-proton collision which, following the standard notation, can be written as

$$\sigma_{had} = 2 \int_0^1 d\tau \hat{\sigma}(S_{had}\tau) \int_\tau^1 \frac{dx}{x} \sum_q f_q(x) f_{\bar{q}}(\tau/x), \quad (15)$$

where the sum is over the parton distribution functions of all the light quarks inside the proton and the symmetry factor of two appears due to the interchange of the two partons in the initial state. In order to calculate the partonic cross section we need to know the  $\text{Im}[M^2(\hat{s})]$  which, using the Cutkosky rules, can be written as,

$$-\text{Im}[M^2(\hat{s})] = \frac{1}{2} \sum_f \int d\Pi_f |\mathcal{M}(\rho \rightarrow f)|^2, \quad (16)$$

where  $\mathcal{M}(p \rightarrow f)$  is the matrix element of the process [ $\rho \rightarrow$  final state  $f$ ] assuming that  $\rho$  has a mass  $p^2 = \hat{s}$  and  $d\Pi_f$  is the corresponding phase space factor. For example, assuming that the resonance  $\rho$  only decays to  $\bar{\chi}_1 \chi_2$  fermions states the corresponding  $\text{Im}[M^2(\hat{s})]$  can be written as,

$$\text{Im}[M^2(\hat{s})]_{\bar{\chi}_1 \chi_2} = -\frac{g_{dec}^2}{24\pi\hat{s}} \theta(\sqrt{\hat{s}} - m_{\chi_1} - m_{\chi_2}) [(\hat{s} - (m_{\chi_1} + m_{\chi_2})^2)(\hat{s} - (m_{\chi_1} - m_{\chi_2})^2)]^{1/2} \times \left\{ (1 + |a_{12}|^2) \left[ \hat{s} - \frac{\hat{s}(m_{\chi_1}^2 + m_{\chi_2}^2) + (m_{\chi_1}^2 - m_{\chi_2}^2)^2}{2\hat{s}} \right] + 3m_{\chi_1} m_{\chi_2} (1 - |a_{12}|^2) \right\}. \quad (17)$$

In order to understand the effect of finite width of the composite gluon in a more quantitative way we consider a simplified model where the  $\rho$  exclusively decays into the  $\bar{\chi}\chi$  pair of composite resonances with the mass  $m_\chi$ . With this assumption, we compute the true production cross section as well as the one using fixed width approximation. The results are presented in the Table 2 and the Fig. 5, where we show the differential cross section as a function of the invariant mass of the fermion pair. One can observe that the narrow width approximation is reproducing neither the shape nor the the integrated production cross section once the narrow resonance limit,  $\Gamma_\rho \ll M_\rho$ , is not satisfied. Another region where the narrow width approximation fails is near the threshold  $2m_\chi = M_\rho$ . This can be understood by noticing that the total width vanishes above this threshold (i.e.,  $2m_\chi > M_\rho$ ) unlike  $\text{Im}[M^2(\hat{s})]$ .

## C Minimal composite Higgs model M4<sub>5</sub>

In this section we briefly review the minimal composite Higgs model (we urge the interested readers to refer to the original literatures [8,41] for more details) which is based on the  $SO(5)/SO(4)$  symmetry breaking pattern.

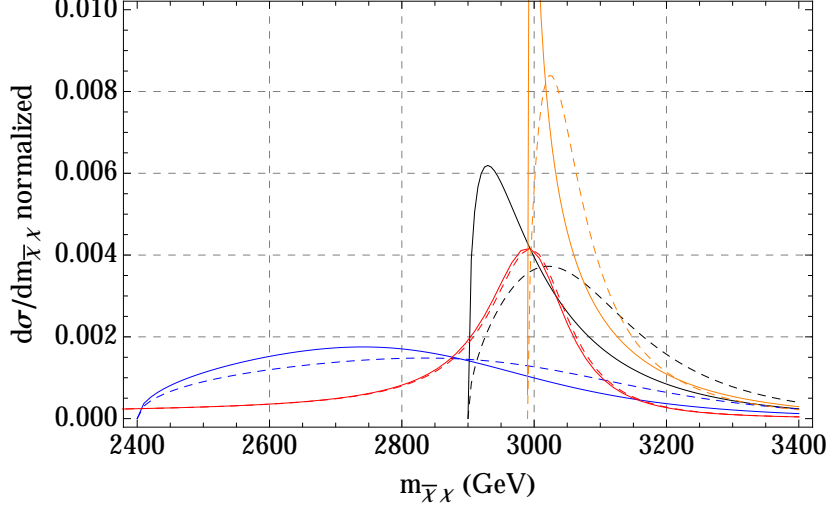


Figure 5: Normalized differential cross section as a functions of the invariant mass of the fermion pair, for  $\sqrt{S_{had}} = 8$  TeV collisions. The black, blue, red and orange lines correspond to the reference points A, B, C and D respectively defined in table 2. While the solid lines correspond to the true cross section, the dashed lines correspond to the fixed width approximation.

In this paper we consider the composite gluon extension of the  $M4_5$  phenomenological model presented in [41]. The interaction between top quarks and composite fermions can be parametrized as

$$\mathcal{L}^{M4_5} \supset -M_Q \bar{Q}Q + yf(\bar{\Psi}_L)^I U_{Ii} Q_R^i + yc_2 f(\bar{\Psi}_L)^I U_{I5} t_R^5 \quad (18)$$

where  $Q$  is a multiplet (4-plet of  $SO(4)$ ) of the composite top partners,

$$Q = \frac{1}{\sqrt{2}} \begin{pmatrix} iB_{1/3} - iX_{5/3} \\ B_{1/3} + X_{5/3} \\ iT_{2/3}^1 + iT_{2/3}^2 \\ -T_{2/3}^1 + T_{2/3}^2 \end{pmatrix} \quad (19)$$

and  $\Psi_L$  and  $t_R$  stand for the SM fermions which are embedded into incomplete multiplets of  $SO(5)$  namely,

$$\Psi = \frac{1}{\sqrt{2}} \begin{pmatrix} ib_L \\ b_L \\ it_L \\ -t_L \\ 0 \end{pmatrix}, \quad t_R^5 = \begin{pmatrix} 0 \\ 0 \\ 0 \\ 0 \\ t_R \end{pmatrix}. \quad (20)$$

The  $5 \times 5$  matrix  $U$  containing the goldstone Higgs is given by (in the unitary gauge),

$$U = \begin{pmatrix} \mathbb{1}_3 & & \\ & \cos \frac{h}{f} & \sin \frac{h}{f} \\ & -\sin \frac{h}{f} & \cos \frac{h}{f} \end{pmatrix}. \quad (21)$$

The masses of the charge 5/3 and  $-1/3$  particles are given by,  $M_{1/3} = \sqrt{M_Q^2 + y^2 f^2}$  and  $M_{5/3} = M_Q$  respectively. The masses of the charge 2/3 fermions are given by the  $3 \times 3$  matrix

$$\begin{pmatrix} \frac{c_2 y f}{\sqrt{2}} \sin \frac{v}{f} & y f \cos^2 \frac{v}{2f} & y f \sin^2 \frac{v}{2f} \\ 0 & -M_Q & 0 \\ 0 & 0 & -M_Q \end{pmatrix}, \quad (22)$$

where the lightest field is the SM top quark and the other two fermions have the masses  $M_{1,2/3} = M_Q$ ,  $M_{2,2/3} = \sqrt{M_Q^2 + y^2 f^2} (1 + \mathcal{O}(v^2/f^2))$ . The strength of the mixing between elementary and composite fields can be parametrized by the mixing angle

$$s_L \equiv \sin \theta_L = \frac{y f}{\sqrt{y^2 f^2 + M_Q^2}}. \quad (23)$$

Extension of this setup by composite gluons was presented in [40] and the relevant part of the Lagrangian is given by

$$\mathcal{L}_{QCD} = -\frac{1}{4} \rho_{\mu\nu}^2 + \frac{F^2}{2} (g_* \rho_\mu^* - g A_\mu^*)^2 + g \bar{\mathcal{E}} \gamma^\mu \mathcal{E} A_\mu^* + g_* \bar{\mathcal{C}} \gamma^\mu \mathcal{C} \rho_\mu^*, \quad (24)$$

where  $A^*$  and  $\rho^*$  are the elementary and composite gluons respectively and  $\mathcal{C}, \mathcal{E}$  denote generic composite and elementary fermion fields. One can now find the mass eigenstates corresponding to the SM gluon  $A_\mu$  and its partner  $\rho_\mu$ ,

$$\rho_\mu = \frac{g_* \rho_\mu^* - g A_\mu^*}{\sqrt{g^2 + g_*^2}}, \quad A_\mu = \frac{g \rho_\mu^* + g_* A_\mu^*}{\sqrt{g^2 + g_*^2}}. \quad (25)$$

The QCD interaction is given by the term

$$\frac{g g_*}{\sqrt{g^2 + g_*^2}} A_\mu (\bar{\mathcal{C}} \gamma_\mu \mathcal{C} + \bar{\mathcal{E}} \gamma_\mu \mathcal{E}) \quad (26)$$

which gives,

$$g_{QCD} = \frac{g g_*}{\sqrt{g^2 + g_*^2}} \approx g \text{ in the limit } g \ll g_*. \quad (27)$$

The couplings of the elementary and composite fermions to the heavy gluon can be written as

$$\begin{aligned} & \rho_\mu \left( \sqrt{g_*^2 - g_{QCD}^2} \bar{\mathcal{C}} \gamma^\mu \mathcal{C} - \frac{g_{QCD}^2}{\sqrt{g_*^2 - g_{QCD}^2}} \bar{\mathcal{E}} \gamma^\mu \mathcal{E} \right) \\ & \approx \rho_\mu \left( g_* \bar{\mathcal{C}} \gamma_\mu \mathcal{C} - \frac{g_{QCD}^2}{g_*} \bar{\mathcal{E}} \gamma_\mu \mathcal{E} \right). \end{aligned} \quad (28)$$

Eq. 28 reveals that the composite gluon interacts with the composite fermion resonances with strength  $\sim g_*$ . Moreover, they will interact strongly also with the third generation SM fermions due to their strong mixing with the composite sector. The rest of the SM fermions couples to  $\rho$  with a suppressed strength  $g^2/g_*$ .



## References

- [1] G. Aad *et al.* [ATLAS Collaboration], Phys. Lett. B **716** (2012) 1 [[arXiv:1207.7214](#) [hep-ex]].
- [2] S. Chatrchyan *et al.* [CMS Collaboration], Phys. Lett. B **716** (2012) 30 [[arXiv:1207.7235](#) [hep-ex]].
- [3] D. B. Kaplan and H. Georgi, *SU(2) × U(1) Breaking by Vacuum Misalignment*, Phys.Lett. **B136** (1984) 183.
- [4] H. Georgi and D. B. Kaplan, *Composite Higgs and Custodial SU(2)*, Phys.Lett. **B145** (1984) 216.
- [5] R. Contino, Y. Nomura and A. Pomarol, Nucl. Phys. B **671** (2003) 148 [[hep-ph/0306259](#)].
- [6] B. Bellazzini, C. Csaki and J. Serra, Eur. Phys. J. C **74** (2014) 5, 2766 [[arXiv:1401.2457](#) [hep-ph]].
- [7] D. B. Kaplan, Nucl. Phys. B **365** (1991) 259.
- [8] K. Agashe, R. Contino and A. Pomarol, Nucl. Phys. B **719** (2005) 165 [[hep-ph/0412089](#)].
- [9] A. Pomarol and F. Riva, JHEP **1208** (2012) 135 [[arXiv:1205.6434](#) [hep-ph]].
- [10] O. Matsedonskyi, G. Panico and A. Wulzer, JHEP **1301** (2013) 164 [[arXiv:1204.6333](#) [hep-ph]].
- [11] D. Marzocca, M. Serone and J. Shu, JHEP **1208**, 013 (2012) [[arXiv:1205.0770](#) [hep-ph]].
- [12] S. De Curtis, M. Redi and A. Tesi, JHEP **1204** (2012) 042 [[arXiv:1110.1613](#) [hep-ph]].
- [13] G. Panico, M. Redi, A. Tesi and A. Wulzer, JHEP **1303**, 051 (2013) [[arXiv:1210.7114](#) [hep-ph]].
- [14] S. Chatrchyan *et al.* [CMS Collaboration], Phys. Lett. B **729** (2014) 149 [[arXiv:1311.7667](#) [hep-ex]].
- [15] G. Aad *et al.* [ATLAS Collaboration], JHEP **1411** (2014) 104 [[arXiv:1409.5500](#) [hep-ex]].
- [16] J. Barnard, T. Gherghetta, A. Medina and T. S. Ray, JHEP **1310** (2013) 055 [[arXiv:1307.4778](#) [hep-ph]].
- [17] C. Csaki, A. Falkowski and A. Weiler, JHEP **0809** (2008) 008 [[arXiv:0804.1954](#) [hep-ph]].
- [18] K. Agashe, A. Azatov and L. Zhu, Phys. Rev. D **79** (2009) 056006 [[arXiv:0810.1016](#) [hep-ph]].
- [19] M. Blanke, A. J. Buras, B. Duling, S. Gori and A. Weiler, JHEP **0903** (2009) 001 [[arXiv:0809.1073](#) [hep-ph]].
- [20] S. Casagrande, F. Goertz, U. Haisch, M. Neubert and T. Pfoh, JHEP **0810**, 094 (2008) [[arXiv:0807.4937](#) [hep-ph]].
- [21] G. Cacciapaglia, C. Csaki, J. Galloway, G. Marandella, J. Terning and A. Weiler, JHEP **0804**, 006 (2008) [[arXiv:0709.1714](#) [hep-ph]].
- [22] A. L. Fitzpatrick, G. Perez and L. Randall, Phys. Rev. Lett. **100**, 171604 (2008) [[arXiv:0710.1869](#) [hep-ph]].
- [23] J. Santiago, JHEP **0812** (2008) 046 [[arXiv:0806.1230](#) [hep-ph]].
- [24] C. Csaki, A. Falkowski and A. Weiler, Phys. Rev. D **80** (2009) 016001 [[arXiv:0806.3757](#) [hep-ph]].

- [25] C. Delaunay, O. Gedalia, S. J. Lee, G. Perez and E. Ponton, Phys. Rev. D **83** (2011) 115003 [[arXiv:1007.0243](#) [hep-ph]].
- [26] M. Redi and A. Weiler, JHEP **1111** (2011) 108 [[arXiv:1106.6357](#) [hep-ph]].
- [27] M. Carena, A. D. Medina, B. Panes, N. R. Shah and C. E. M. Wagner, Phys. Rev. D **77** (2008) 076003 [[arXiv:0712.0095](#) [hep-ph]].
- [28] The ATLAS collaboration, ATLAS-CONF-2013-051, ATLAS-COM-CONF-2013-055.
- [29] S. Chatrchyan *et al.* [CMS Collaboration], Phys. Rev. Lett. **112**, 171801 (2014) [[arXiv:1312.2391](#) [hep-ex]].
- [30] M. Chala, J. Juknevič, G. Perez and J. Santiago, JHEP **1501** (2015) 092 [[arXiv:1411.1771](#) [hep-ph]].
- [31] K. Agashe, A. Belyaev, T. Krupovnickas, G. Perez and J. Virzi, Phys. Rev. D **77** (2008) 015003 [[hep-ph/0612015](#)].
- [32] B. Lillie, L. Randall and L. T. Wang, JHEP **0709** (2007) 074 [[hep-ph/0701166](#)].
- [33] B. Lillie, J. Shu and T. M. P. Tait, Phys. Rev. D **76** (2007) 115016 [[arXiv:0706.3960](#) [hep-ph]].
- [34] C. Bini, R. Contino and N. Vignaroli, JHEP **1201** (2012) 157 [[arXiv:1110.6058](#) [hep-ph]].
- [35] K. Kong, M. McCaskey and G. W. Wilson, JHEP **1204** (2012) 079 [[arXiv:1112.3041](#) [hep-ph]].
- [36] N. Vignaroli, [arXiv:1504.01768](#) [hep-ph].
- [37] D. Greco and D. Liu, JHEP **1412** (2014) 126 [[arXiv:1410.2883](#) [hep-ph]].
- [38] M. Backovic, G. Perez, T. Flacke and S. J. Lee, [arXiv:1409.0409](#) [hep-ph].
- [39] A. Azatov, M. Salvarezza, M. Son and M. Spannowsky, Phys. Rev. D **89** (2014) 7, 075001 [[arXiv:1308.6601](#) [hep-ph]].
- [40] R. Contino, T. Kramer, M. Son and R. Sundrum, JHEP **0705**, 074 (2007) [[hep-ph/0612180](#)].
- [41] A. De Simone, O. Matsedonskyi, R. Rattazzi and A. Wulzer, JHEP **1304**, 004 (2013) [[arXiv:1211.5663](#) [hep-ph]].
- [42] K. Agashe, R. Contino, L. Da Rold and A. Pomarol, Phys. Lett. B **641**, 62 (2006) [[hep-ph/0605341](#)].
- [43] O. Matsedonskyi, G. Panico and A. Wulzer, JHEP **1412**, 097 (2014) [[arXiv:1409.0100](#) [hep-ph]].
- [44] T. Gherghetta and A. Pomarol, Nucl. Phys. B **586**, 141 (2000) [[hep-ph/0003129](#)].
- [45] A. Azatov, G. Panico, G. Perez and Y. Soreq, JHEP **1412**, 082 (2014) [[arXiv:1408.4525](#) [hep-ph]].
- [46] A. Djouadi, G. Moreau and F. Richard, Phys. Lett. B **701**, 458 (2011) [[arXiv:1105.3158](#) [hep-ph]].
- [47] R. Barcelo, A. Carmona, M. Masip and J. Santiago, Phys. Lett. B **707** (2012) 88 [[arXiv:1106.4054](#) [hep-ph]]. and
- [48] R. Barcelo, A. Carmona, M. Chala, M. Masip and J. Santiago, Nucl. Phys. B **857** (2012) 172 [[arXiv:1110.5914](#) [hep-ph]].

- [49] A. Alloul, N. D. Christensen, C. Degrande, C. Duhr and B. Fuks, *Comput. Phys. Commun.* **185** (2014) 2250 [[arXiv:1310.1921](#) [hep-ph]].
- [50] J. Alwall, R. Frederix, S. Frixione, V. Hirschi, F. Maltoni, O. Mattelaer, H.-S. Shao and T. Stelzer *et al.*, *JHEP* **1407** (2014) 079 [[arXiv:1405.0301](#) [hep-ph]].
- [51] T. Sjostrand, S. Mrenna and P. Z. Skands, *JHEP* **0605** (2006) 026 [[hep-ph/0603175](#)].
- [52] T. Sjostrand, S. Mrenna and P. Z. Skands, *Comput. Phys. Commun.* **178** (2008) 852 [[arXiv:0710.3820](#) [hep-ph]].
- [53] J. Pumplin, D. R. Stump, J. Huston, H. L. Lai, P. M. Nadolsky and W. K. Tung, *JHEP* **0207** (2002) 012 [[hep-ph/0201195](#)].
- [54] G. Aad *et al.* [ATLAS Collaboration], [arXiv:1503.05425](#) [hep-ex].
- [55] M. Cacciari, G. P. Salam and G. Soyez, *Eur. Phys. J. C* **72** (2012) 1896 [[arXiv:1111.6097](#) [hep-ph]].
- [56] M. Cacciari, G. P. Salam and G. Soyez, *JHEP* **0804** (2008) 063 [[arXiv:0802.1189](#) [hep-ph]].
- [57] Y. L. Dokshitzer, G. D. Leder, S. Moretti and B. R. Webber, *JHEP* **9708** (1997) 001 [[hep-ph/9707323](#)].
- [58] M. Aliev, H. Lacker, U. Langenfeld, S. Moch, P. Uwer and M. Wiedermann, *Comput. Phys. Commun.* **182**, 1034 (2011) [[arXiv:1007.1327](#) [hep-ph]].
- [59] M. Cacciari, S. Frixione, M. L. Mangano, P. Nason and G. Ridolfi, *JHEP* **0809**, 127 (2008) [[arXiv:0804.2800](#) [hep-ph]].
- [60] S. Chatrchyan *et al.* [CMS Collaboration], *Phys. Rev. Lett.* **111** (2013) 21, 211804 [Erratum-ibid. **112** (2014) 11, 119903] [[arXiv:1309.2030](#) [hep-ex]].
- [61] The ATLAS collaboration, “A search for  $t\bar{t}$  resonances in the lepton plus jets final state with ATLAS using 14 inverse fb of pp collisions at  $\sqrt{s} = 8$  TeV,” ATLAS-CONF-2013-052, ATLAS-COM-CONF-2013-052.
- [62] A. Avetisyan and T. Bose, [arXiv:1309.2234](#) [hep-ex].
- [63] S. Chatrchyan *et al.* [CMS Collaboration], *JHEP* **1303** (2013) 037 [Erratum-ibid. **1307** (2013) 041] [[arXiv:1212.6194](#) [hep-ex]].
- [64] The ATLAS collaboration, ATLAS-CONF-2013-065, ATLAS-COM-CONF-2013-065.
- [65] D. E. Kaplan, K. Rehermann, M. D. Schwartz and B. Tweedie, *Phys. Rev. Lett.* **101** (2008) 142001 [[arXiv:0806.0848](#) [hep-ph]].
- [66] S. Biswas, D. Ghosh and S. Niyogi, *JHEP* **1406** (2014) 012 [[arXiv:1312.0549](#) [hep-ph]].
- [67] J. M. Butterworth, A. R. Davison, M. Rubin and G. P. Salam, *Phys. Rev. Lett.* **100** (2008) 242001 [[arXiv:0802.2470](#) [hep-ph]].
- [68] P. Byakti and D. Ghosh, *Phys. Rev. D* **86** (2012) 095027 [[arXiv:1204.0415](#) [hep-ph]].